PAPER • **OPEN ACCESS**

Experimental research and the numerical simulation of the non-standard pump for the flow-circulation type reactor

To cite this article: A P Khomyakov *et al* 2019 *IOP Conf. Ser.: Mater. Sci. Eng.* **537** 062060

IOP Conf. Series: Materials Science and Engineering **537** (2019) 062060 doi:10.1088/1757-899X/537/6/062060

Experimental research and the numerical simulation of the non-standard pump for the flow-circulation type reactor

A P Khomyakov[1], S V Mordanov[1], V A Nikulin[1], M N Beloded[2] and P A Shkurin[2]

[1]The department of chemical plant machinery and equipment, Institute of Chemical Engineering, Ural Federal University, Ekaterinburg, Russia
[2]SverdNIIhimmash JSC, Ekaterinburg, Russia

E-mail: s.v.mordanov@urfu.ru

Abstract. The paper shows the results of the experimental measurements and the numerical simulation of the flow-circulation type reactor pump main characteristics. The mathematical model based on Navier-Stokes equations and standard k-epsilon turbulence model was used for the pump CFD simulation. The pump power consumption was calculated by the proposed CFD post-processing method. It is found that the simulation error of the proposed method is not more than 2.9%. The obtained results include the regression equations of the pump full pressure, the pump feed and the power consumption at the pump cross-points.

1. Introduction

A flow-circulation type technological line usually consists of a circulation pump, a flow type reactor, ancillary equipment, and pipelines. The reaction apparatus can be small volume vessels [1, 2], shell or tube heat exchangers [3], jet reactors [4] and contact devices with packings or Venturi tubes [5]. A hydrodynamic mode of a flow-circulation type technological line significantly depends on circulation pump characteristics. The main characteristics of a circulation pump are the pump flow, the pump pressure (the pump head), and the power consumption. These characteristics are extremely important when designing a technological line, especially when it is impossible to use a standard pump for one reason or another.

This paper is focused on the experimental research and the numerical simulation of the main characteristics of the axial-centrifugal non-standard circulation pump.

2. Experimental research

Figure 1 shows the scheme of the experimental test-stand. The experimental test-stand consists of the axial-centrifugal non-standard circulation pump *1*, the reactor vessel *2*, the flexible pipeline *3*, the initial solution tank *4*, the spent solution tank *5*, the manometer *P*, the flow meter *F*, and the level gauges *L*.

Figure 2 shows the circulation pump scheme. The pump rotor consists of the small pitch auger *1* in the entrance of the receiving chamber, the large pith auger *2* in the main part, and the impeller *3* in the pump discharge chamber. The crosspiece *4* is designed to prevent a swirling flow outside the auger chamber.

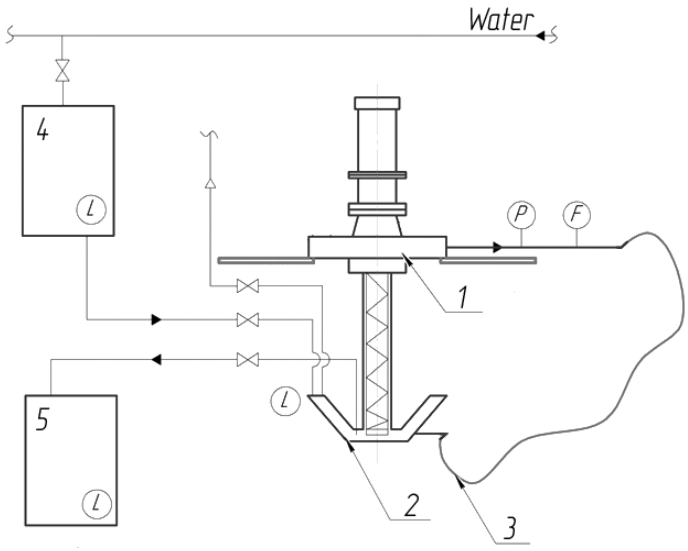

Figure 1. Scheme of the experimental test-stand: *1* – circulation pump, *2* – reactor vessel, *3* – flexible pipeline, *4* – initial solution tank, *5* – spent solution tank, *P* – manometer, *F* – flow meter, *L* – level gauges.

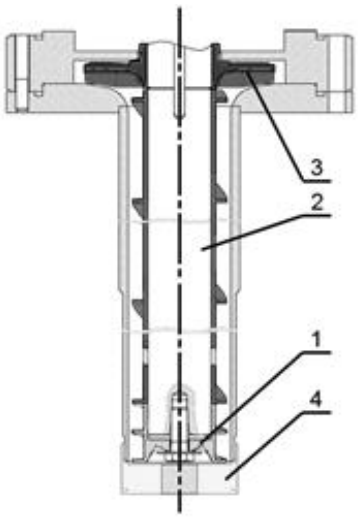

Figure 2. Scheme of the circulation pump: *1* – small pitch auger, *2* – large pitch auger, *3* – impeller, *4* – crosspiece.

The water from the initial solution tank *4* enters the reactor vessel *2* and fills the circulation contour consisting of the pump *1*, the reactor vessel *2* and the flexible pipe *3*. Then, the water supply line overlaps and pump 1 starts.

The flow of the pump *1* is controlled by the rotor speed. The rotor speed varies in the range of 750-1500 rpm. The pump flow and pressure are measured by flow meter *F* and manometer *P* for each pump operation mode. After the measurements water from the circulation contour exits to the spent solution tank 5.

3. Numerical simulation

The mathematical model based on Navier-Stokes equations and standard k-epsilon turbulence model was used for pump CFD simulation. For steady-state isothermal conditions Navier-Stokes equations takes form [6]:

$$\mathrm{div}(\rho\vec{u})=0, \tag{1}$$

$$(\rho u_j)\frac{\partial u_i}{\partial x_j}=\frac{\mathrm{d}p}{\mathrm{d}x_i}+\frac{\partial}{\partial x_j}\left[\mu\left(\frac{\partial u_j}{\partial x_i}+\frac{\partial u_i}{\partial x_j}-\frac{2}{3}\delta_{ij}\frac{\partial u_i}{\partial x_i}\right)\right]+\rho g_i. \tag{2}$$

There ρ is the density, kg/m^3; u is the velocity, m/s; i, j are the indexes of the longitudinal and the transverse directions of the flow; x is the coordinate, m; p is the pressure, Pa; μ is the viscosity, Pa·s; δ_{ij} is the metric tensor; g is the gravity force acceleration, m/s^2.

Standard k-epsilon turbulence model [7] for the steady-state isothermal conditions takes form:

$$\frac{\partial}{\partial x_i}(\rho k u_i)=\frac{\partial}{\partial x_j}\left[\left(\mu+\frac{\mu_t}{\sigma_k}\right)\frac{\partial k}{\partial x_j}\right]+G_k-\rho\varepsilon, \tag{3}$$

$$\frac{\partial}{\partial x_i}(\rho\varepsilon u_i)=\frac{\partial}{\partial x_j}\left[\left(\mu+\frac{\mu_t}{\sigma_\varepsilon}\right)\frac{\partial \varepsilon}{\partial x_j}\right]+C_{1\varepsilon}G_k-C_{2\varepsilon}\rho\frac{\varepsilon^2}{k}, \tag{4}$$

$$G_k=\mu_t S^2, \tag{5}$$

$$S\equiv(2S_{ij}S_{ij})^{0.5}, \tag{6}$$

$$S_{ij}=\frac{1}{2}\left(\frac{\partial u_j}{\partial x_i}+\frac{\partial u_i}{\partial x_j}\right), \quad (7)$$

$$\mu_t=\rho C_\mu \frac{k^2}{\varepsilon}. \quad (8)$$

There k is the specific turbulent kinetic energy, J/kg; μ_t is the turbulent viscosity, Pa·s; G_k is the turbulent kinetic energy generation due to the average flow gradient, J/(m^3·s); ε is the specific turbulent kinetic energy dissipation, J/(kg·s); S is the viscous stress tensor module, s^{-1}; S_{ij} is the viscous stress tensor, s^{-1}. The values of the model constants were taken according to Marshall and Bakker [8]: $C_{1\varepsilon}$ = 1.44, $C_{2\varepsilon}$ = 1.92, σ_k = 1.0, σ_ε = 1.3, C_μ = 0.09.

The pump power consumption was calculated by the CFD post-processing method proposed for a mechanical mixing power consumption estimation [9], this post-processing method was not used for a pump simulation previously. According to the offered method the pump power consumption was calculated by the equations:

$$N_{useful}=\omega \int_0^S M_i^* \mathrm{d}S = \omega \int_0^S p_{din_i} r_i \mathrm{d}S = \frac{2\pi n}{60} \int_0^S \frac{\rho u_i^2}{2} \sqrt{x_i^2+y_i^2}\,\mathrm{d}S, \quad (9)$$

$$N=k_\delta \frac{N_{useful}}{\eta}, \quad (10)$$

$$\eta=\Pi_{j=1}^{n}\eta_j. \quad (11)$$

There N_{useful} is the useful power consumption, W; ω is the rotor angular velocity, rad/s; i is the index of the rotor area unit; M_i^* is the specific torque, N·m/m^2; p_{dyn} is the dynamic pressure, Pa; r is the radius vector, m; S is the rotor working surface area, m^2; n is the rotor speed, rpm; x, y are the coordinates, m; N is the total power consumption, W; k_δ is the empirical error coefficient; η is the pump drive efficiency; η_j is the pump drive element efficiency. The error coefficient k_δ was taken to be 1.12 according to the practical experience.

4. Results and Discussion

Table 1 shows the measured and calculated pump feed relevant to the pump cross-points pressure. The measured values were obtained by the experiments on the test-stand (figure 1), the calculated values were obtained by the ANSYS Fluent code CFD simulation using equations (1) – (8) and the regular mesh with about 400 thousand polyhedral elements. The cross-points feed calculation error varies in the range of 0.2-2.9%. The average calculation error is 1.5%. Thus, the equations (1) – (8) can be used for non-standard pumps CFD simulation using low density meshes.

Table 1. Measured and calculated pump feed.

Rotor speed, rpm	Pressure, bar	Feed, m^3/h		Calculation error, %
		Measurement	Calculation	
750	0.06	6.80	6.60	2.9
1000	0.16	9.10	8.93	1.9
1250	0.28	11.30	11.09	1.9
1410	0.38	12.70	12.67	0.2
1500	0.45	13.50	13.57	0.5

Figure 3 shows the dependence of the measured and calculated pump feed on the rotor speed. The pump feed increases almost linearly with increasing the rotor speed. The pump feed varies in the range of 6.8-13.5 m^3/h for the considered rotor speed interval.

Figure 4 shows the dependence of the measured and calculated pump pressure on the rotor speed. The pump pressure increases nonlinearly with increasing the rotor speed. The pump pressure varies in the range of 0.06-0.45 bar for the considered rotor speed interval.

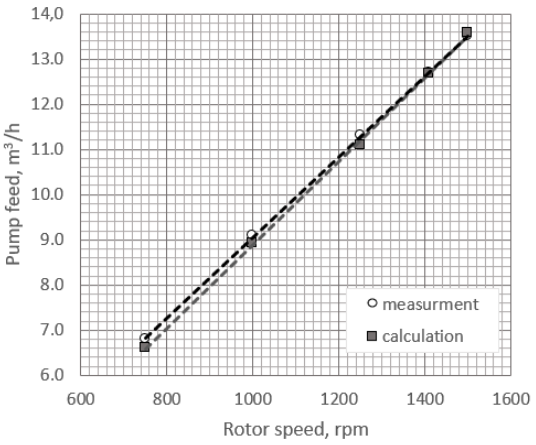

Figure 3. Dependence of the measured and calculated pump feed on the rotor speed.

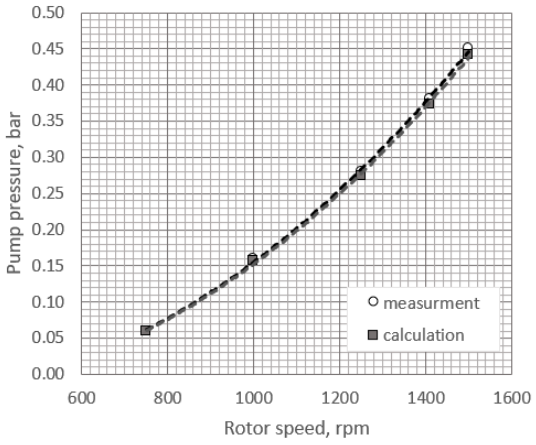

Figure 4. Dependence of the measured and calculated pump pressure on the rotor speed.

The nature of shown changes of the pump feed and the pressure with the rotor speed change corresponds well to the characteristics of typical centrifugal pumps [10].

Figure 5 shows the dependence of measured and calculated pump power consumption on the rotor speed. The power consumption depends on the rotor speed to the second degree. The pump power consumption varies in the range of 0.46-1.76 kW for the considered rotor speed interval. The value of the total power consumption calculation error is not more than 7.2% for the considered rotor speed interval, the average calculation error is 3.9%. Thus, the offered CFD post-processing method can be used for a centrifugal pump power consumption calculation.

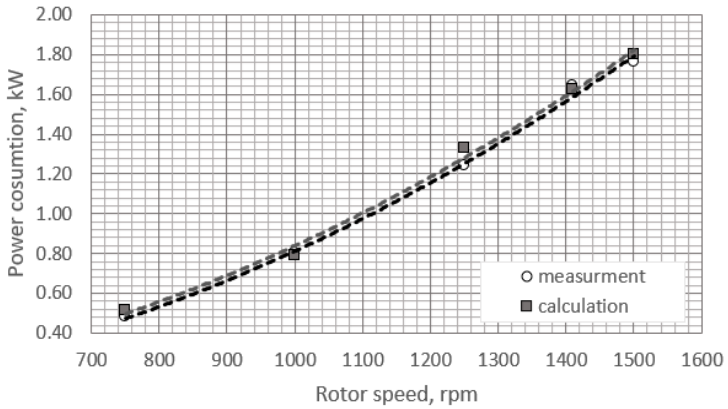

Figure 5. Dependence of the measured and calculated pump power consumption on the rotor speed.

The regressive equations (12) – (15) for the values of the pump pressure, the pump feed and the total power consumption were obtained based on the joint analysis of the measurement and simulation results. The approximation error of the pump main characteristics equations (12) – (15) is not more than 0.5%. Thus, the proposed equations (12) – (15) can be used for a flow-circulation type technological lines design and research.

$$P = 0.0032 \cdot Q^2 - 0.0092 \cdot Q - 0.0225, \quad (12)$$

$$Q = 0.0091 \cdot n - 0.0909, \quad (13)$$

$$P = (0.0003 \cdot n^2 - 0.1146 \cdot n - 8.4768) \cdot 10^{-3}, \quad (14)$$

$$N = (0.0008 \cdot n^2 - 0.0382 \cdot n - 64.155) \cdot 10^{-3}, \quad (15)$$

There *P* is the pump pressure, bar; *Q* is the pump feed, m^3/h; *n* is the rotor speed, rpm; *N* is the pump total power consumption, kW.

5. Conclusion

We have obtained experimental and calculated dependences of the pump feed on the pump pressure at given rotator speed. The average pump feed CFD calculation error is 1.5%. Thus, the proposed mathematical model can be used for a non-standard pump CFD simulation.

We have obtained experimental and calculated dependences of the pump feed and the pump pressure on the rotor speed. It is shown, that the dependence of the pump feed on the rotor speed is linear and the dependence of the pump pressure is nonlinear on the considered rotor speed interval. The pump feed varies in the range of 6.8-13.5 m3/h. The pump pressure varies in the range of 0.06-0.45 bar. The nature of the dependences of the pump feed and the pressure on the rotor speed corresponds well to the characteristics of typical centrifugal pumps.

The experimental and calculated dependences of the pump power consumption on the rotor speed were obtained. It is shown, that the pump power consumption varies in the range of 0.46-1.76 kW for the considered rotor speed interval. The average value of the total power consumption calculation error is 3.9%. Thus, the proposed CFD post-processing method can be used for a centrifugal pump power consumption calculation.

The regression equations for the main characteristics of the axial-centrifugal non-standard circulation pump were obtained. The approximation error value of the pump main characteristics equations is not more than 0.5%. Thus, this equation can be used for design and research of flow-circulation type technological lines.

References

[1] Blenke H 1979 Loop reactors *Adv. Biochem. Eng.* **13** 121-4
[2] Tesser R, Casale L, Verde D, Serio M Di and Santacesaria E 2009 Batch and loop reactor modeling. *Chem. Eng. J* **154** 25-33
[3] Tanaka M 1990 Suspension Polymerization of Styrene with Circular Loop Reactor *Journal of Applied Polymer Science* **39** 955-66
[4] Warmeling H, Behr A and Vorholt A J 2016 Jet loop reactors as a versatile reactor set up - Intensifying catalic reactions: A review *Chem. Eng. Sci.* **149** 229-48
[5] Heiswolf J J, Engelvaart L B, van den Eijnden M G, Kreutzer M T, Kapteijn F and Moulijn J A 2001 Hydrodynamic aspects of the monolith loop reactor *Chem. Eng. Sci.* **56** 805-12
[6] Landau L D and Lifshitz E M 1986 *Fluid Mechanics: Volume 6 of Cource of Theoretical Physics* (Oxford: Pergamon Press)
[7] Wilcox D C 2006 *Turbulence Modeling for CFD* (San Diego: DCW Industries)
[8] Marshall E M and Bakker A 2003 *Computational Fluid Mixing* (Lebanon: Fluent Inc.)
[9] Khomyakov A P, Nikulin V A, Mordanov S V, Korchenkin K K and Melentyev A B 2015 Increasing the Efficiency of Chemical Composition Homogenization for Nitric Acid Uranium Solutions. Part 2: Additional Mechanical Mixing Application *Journal of Radiation Safety* **2(46)** 38-45
[10] Stewart M 2019 *Surface Production Operations: Pumps and Compressors. Volume IV* (Cambridge: Gulf Professional Publishing)